

# Dalton Transactions

Accepted Manuscript



This is an *Accepted Manuscript*, which has been through the Royal Society of Chemistry peer review process and has been accepted for publication.

*Accepted Manuscripts* are published online shortly after acceptance, before technical editing, formatting and proof reading. Using this free service, authors can make their results available to the community, in citable form, before we publish the edited article. We will replace this *Accepted Manuscript* with the edited and formatted *Advance Article* as soon as it is available.

You can find more information about *Accepted Manuscripts* in the [Information for Authors](#).

Please note that technical editing may introduce minor changes to the text and/or graphics, which may alter content. The journal's standard [Terms & Conditions](#) and the [Ethical guidelines](#) still apply. In no event shall the Royal Society of Chemistry be held responsible for any errors or omissions in this *Accepted Manuscript* or any consequences arising from the use of any information it contains.

## COMMUNICATION

## Coexistence of Electrical Conductivity and Ferromagnetism in a Hybrid Material formed from Reduced Graphene Oxide and Manganese Oxide

Cite this: DOI: 10.1039/x0xx00000x

Received 00th January 2012,  
Accepted 00th January 2012Yusuke Murashima,<sup>a</sup> Ryo Ohtani,<sup>a</sup> Takeshi Matsui,<sup>a</sup> Hiroshi Takehira,<sup>a</sup> Ryotaro Yokota,<sup>a</sup> Masaaki Nakamura,<sup>a</sup> Leonard F. Lindoy,<sup>b</sup> and Shinya Hayami<sup>\*a,c,d</sup>

DOI: 10.1039/x0xx00000x

www.rsc.org/

**The coexistence of electrical conductivity and ferromagnetism has been achieved in a reduced graphene oxide/manganese oxide hybrid (rGO-Mn) synthesized by chemical reduction of a graphene oxide and Mn<sup>2+</sup> (as its GO-Mn<sup>2+</sup> complex) using hydrazine. The rGO-Mn and GO-Mn<sup>2+</sup> complexes were characterized by fourier transform infrared spectroscopy (FT-IR), raman spectroscopy, X-ray photoelectron spectroscopy (XPS) and transmission electron microscopy (TEM). In rGO-Mn the Mn was present as manganese oxide nanoparticles located on the rGO nanosheets. This rGO-Mn hybrid exhibits both electrical conductivity and ferromagnetism. The synthesis of hybrids incorporating rGO and metal oxides is proposed as a useful strategy for generation of new multifunctional nano-composite materials.**

The design of multifunctional materials in which electrical conductivity and magnetism coexist has represented an important challenge in material science. So far, only a few materials have been reported that exhibit both metallic conductivity and ferromagnetism,<sup>1</sup> superconductivity and paramagnetism,<sup>2</sup> or superconductivity and ferromagnetism.<sup>3</sup> In a bid to create further difunctional materials of this general type, we have been focusing on the use of the two dimensional nanosheet, reduced graphene oxide (rGO), as one component in the formation of new composites.<sup>4-6</sup>

Graphene (G) has a perfect 2D structure and displays high electrical conductivity.<sup>7-9</sup> rGO, synthesized by reduction of graphene oxide (GO), has a similar 2D structure to GO but, in contrast, has semiconduction properties since many defects are present in its 2D structure.<sup>10-12</sup> rGO has two different types of edges in its sheet structure. The first are armchair edges; these

are not associated with localized spin because they consist of only  $\pi$  and  $\pi^*$  bonds. The second type are zigzag edges which do have localized spins because they are associated with a flat band together with  $\pi$  and  $\pi^*$  bands.<sup>5</sup> The latter defect type thus plays a role in enhancing its magnetic properties<sup>13-15</sup> and, as a consequence, the ferromagnetism of rGO is stronger than that for G. Hence, while rGO does show both electrical conductivity and magnetism, its ferromagnetism is quite weak and needs to be enhanced for practical application.

With respect to the above, we have previously described the synthesis of hybrids of type rGO-M (M = metal oxide) that shows both electrical conductivity and ferromagnetism by reducing GO-metal ion (GO-Fe<sup>3+</sup>, Co<sup>2+</sup>, Ni<sup>2+</sup>) complexes by adding hydrazine and photo irradiation.<sup>6</sup> In the case of rGO-Co and rGO-Ni, the field cooled magnetization (FCM) and zero field cooled magnetization (ZFCM) bifurcated at 11 and 15 K, respectively. For rGO-Fe, on the other hand, the bifurcation occurred at 30 K.

In an extension of this study we now report a new hybrid material based on rGO and ferromagnetic manganese oxide. Reflecting its diverse properties, manganese oxide has been employed for electrodes,<sup>16</sup> catalysts,<sup>17</sup> and soft magnetic materials.<sup>18</sup> It has also been demonstrated that the magnetic behaviour of manganese oxide is sensitive to its particle size and its chemical/physical environment.<sup>19</sup> Consequently, the Curie temperature and coercivity of manganese oxide is anticipated to be changed on hybrid formation with rGO; moreover, the presence of manganese oxide would be expected to influence the conduction behaviour of rGO.

In this study, we report the synthesis of the new rGO-manganese oxide (Mn) hybrid together with an investigation of its electrical conductive and ferromagnetic difunctionality. It was

anticipated that the hybrid would show both electrical conductivity arising from rGO and ferromagnetism from the manganese oxide nanoparticles.

First, GO was prepared by the modified Hummers' method previously reported by us.<sup>20</sup> GO was dispersed in pure water (0.1 g/L) by ultrasonication for 2 h and the resulting GO suspension was centrifuged to remove any aggregated GO. The GO-Mn<sup>2+</sup> complex was synthesized by mixing 100 mL of the GO suspension with 4 mL of manganese acetate tetrahydrate solution (0.1 M) and stirring vigorously at 25 °C for 24 h. Finally, chemical reduction was carried out by refluxing the mixture with 1 mL hydrazine monohydrate at 100 °C for 24 h to yield rGO-Mn as a black residue (Figure 1).

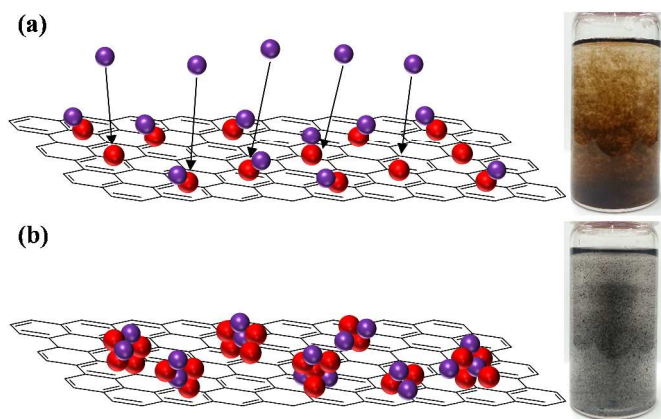


**Figure 1.** Schematic images of the suggested structures of (a) GO-Mn<sup>2+</sup> complex and (b) rGO-Mn along with photographs of the compounds in aqueous suspensions. Violet spheres are manganese ions and red spheres are oxygen atoms.

The rGO-Mn was characterised by fourier transform infrared spectroscopy (FT-IR), raman spectroscopy, X-ray photoelectron spectroscopy (XPS) and transmission electron microscopy (TEM). The FT-IR spectra of GO, GO-Mn<sup>2+</sup> and rGO-Mn were determined (Figure S1). The spectrum of GO showed characteristic bands for O-H, C=O (carboxy and carbonyl), C-OH and C-O-C bonds at 3402, 1735, 1219 and 1049 cm<sup>-1</sup>, respectively.<sup>21, 22</sup> On forming the GO-Mn<sup>2+</sup> complex, the intensity of the O-H peak at 3402 cm<sup>-1</sup> decreased, with the peak broadening due to the loss of interlayer hydrogen bonds between the GO nanosheets by the binding of Mn<sup>2+</sup> ions to the nanosheets. For rGO-Mn, no peaks due to oxygen functional groups were present, with the peak corresponding to the C=C stretching mode of the rGO nanosheets being observed at 1543 cm<sup>-1</sup>.

Raman spectroscopy was employed to investigate the relative domain sizes of the sp<sup>2</sup> and sp<sup>3</sup> carbons in the rGO-Mn sheets (Figure S2). The carbon type was identified by monitoring the G (1580 cm<sup>-1</sup>) and the D (1350 cm<sup>-1</sup>) bands. These G and D bands are assigned to the E<sub>2g</sub> phonon corresponding to sp<sup>2</sup> carbon atoms and the κ-point phonon of A<sub>1g</sub> symmetry for the breathing mode of sp<sup>3</sup> carbon, respectively.<sup>23, 24</sup> The peak ratio (I<sub>D</sub>/I<sub>G</sub>) are 0.882, 0.914, and 1.07 for GO, GO-Mn<sup>2+</sup> complex and rGO-Mn, respectively. The differences in the I<sub>D</sub>/I<sub>G</sub> values demonstrates that the size of the sp<sup>2</sup> domain in GO is decreased in both its derivatives in accord with the formation of rGO from GO through chemical reduction.<sup>25</sup> Furthermore, we measured XPS

spectra for C1s to obtain more detailed information about the nature of the carbon atoms in GO, GO-Mn<sup>2+</sup> complex and rGO-Mn (Figures S3 and S4) using a XPS spectrometer (Thermo Scientific, Sigma Probe) equipped with a vacuum facility at less than 10<sup>-7</sup> Pa. Pure GO nanosheets exhibit two groups of C1s corresponding to composite peaks around 285 and 287 eV (Figure S3). The narrower and higher peak at 287 eV and the broader peak at 285 eV are assigned to oxygenated carbon sites and unoxidized carbon sites, respectively.<sup>26</sup> In the case of the GO-Mn<sup>2+</sup> complex, both groups of peaks were very similar to those of GO, while, after chemical reduction with hydrazine, the intensity of the composite peak around 287 eV decreased, in accord with the loss of the oxygen functional groups (such as epoxy and hydroxyl groups) from GO. However, residual peaks indicated that some epoxy and hydroxyl groups were unaffected by the chemical reduction procedure. This result is in keeping with metal ions attaching to partially negatively charged epoxy and hydroxyl oxygens through electrostatic interaction and inhibiting them from undergoing the reported mechanism for hydrazine reduction of GO.<sup>27</sup>

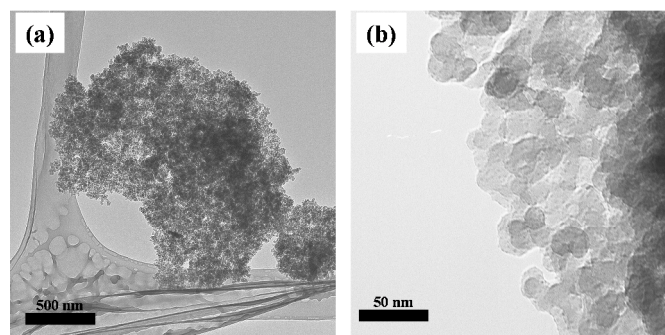


**Figure 2.** TEM image of the rGO-Mn hybrid. (a) overall view of the nanosheet. (b) focused view.

Surface features of rGO-Mn were analyzed from TEM images (Figure 2). Manganese oxide nanoparticles of approximately 10-20 nm were confirmed to be present and to overlap each other on the rGO nanosheets. The formation of nanoparticles parallels the situation that occurs in rGO-Fe and rGO-Co.<sup>6</sup> A possible mechanism for the formation of the nanoparticles involves the loss of oxygen atoms from the GO during the reduction, with these oxygen atoms being trapped by metal ions on the GO leading to the formation of manganese oxide nanoparticles on rGO nanosheets (Figure 1).

Figure 3 shows I-V plots for both the GO-Mn<sup>2+</sup> complex and rGO-Mn. Glass substrates (6×15 mm) for the conductivity measurements were prepared by casting of GO and GO-Mn<sup>2+</sup> complex suspensions in H<sub>2</sub>O of 60 μL and drying at 80 °C three times. Subsequently, substrates with rGO and rGO-Mn were formed by reduction using hydrazine vapor for 24 h at 70 °C. After drying these substrates in vacuum, two electrodes were attached to the substrates with gold paste at a distance of 4 mm. We measured several times and adopted their averaged current values. The GO-Mn<sup>2+</sup> complex shows no conductivity irrespective of the magnitude of applied voltage,<sup>28</sup> while rGO-Mn, on the other hand, shows semiconductive behaviour. A value for the resistance was observed to be higher than that of pristine rGO. This is apparently the result of some oxygen

functional groups surviving after the chemical reduction of GO (as discussed in relation to the XPS analysis), with these acting to block the conduction path in rGO.

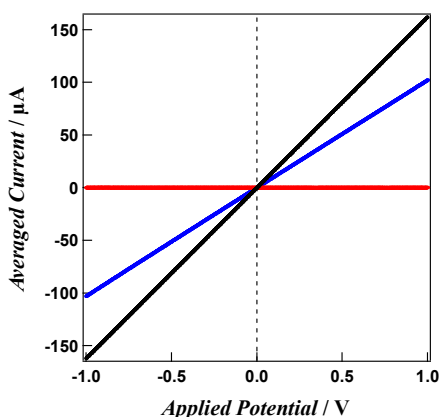


**Figure 3.** Averaged current vs. applied voltage for pristine rGO (black), GO-Mn<sup>2+</sup> complex (red) and rGO-Mn (blue).

Variable temperature magnetic susceptibilities and the field dependency of the magnetization for rGO-Mn were measured with a superconducting quantum interference device (SQUID) magnetometer (Figure 4). FCM and ZFCM bifurcated at 47 K, indicating that rGO-Mn, is, as expected, ferromagnetic. This Curie temperature is very close to the value of 42 K for 10-20 nm sized nanoparticles of Mn<sub>3</sub>O<sub>4</sub> reported by the J. T. Park group.<sup>19</sup> Furthermore, rGO-Mn exhibits magnetic hysteresis at 2 K. The coercivity value is 2700 Oe which is similar to value for bulk Mn<sub>3</sub>O<sub>4</sub> (2650 Oe, 4.2 K).<sup>29</sup> The reported coercivity value of the Mn<sub>3</sub>O<sub>4</sub> nanoparticles was 7600 Oe.<sup>30</sup> This difference in the respective coercivity values very likely originates from an enlargement of the Mn<sub>3</sub>O<sub>4</sub> nanoparticle domains through aggregation on the rGO nanosheets (see TEM discussion) such that their behaviour approaches that of bulk Mn<sub>3</sub>O<sub>4</sub>.

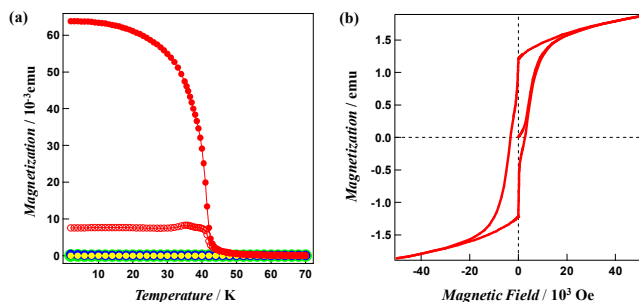


**Figure 4.** Magnetic properties of rGO-Mn. (a) Temperature dependence of FCM for rGO-Mn (red circle), GO (yellow circle), rGO (green circle) and GO-Mn<sup>2+</sup> (blue circle), and ZFCM for rGO-Mn (red open circles) measured at 5 Oe. (b) Field dependence of the magnetization at 2 K.

In conclusion, we have synthesised difunctional rGO-Mn that exhibits the coexistence of electrical conductivity and ferromagnetism. Mn<sub>3</sub>O<sub>4</sub> nanoparticles were formed and aggregated on the rGO sheets. Interestingly, the Curie temperature for the hybrid reflects the nanoparticle nature of the

Mn<sub>3</sub>O<sub>4</sub> while, on the other hand, the coercivity corresponds to that expected for the presence of bulk Mn<sub>3</sub>O<sub>4</sub> on the rGO. These findings represent a novel approach to generating multifunctional nanomaterials derived from conductive nanosheets and various metal oxides. In an extension of this study, we are currently investigating the syntheses of nanomaterials that exhibit magnetic ordering generated from a coupling of magnetic moments of metal ions and conduction electrons of rGO through a Ruderman-Kittel-Kasuya-Yoshida (RKKY) exchange.

## Acknowledgements

This work was supported by Innovative Areas “Coordination Programming” (area 2107) from the MEXT, Japan.

## Notes and references

<sup>a</sup> Department of Chemistry, Graduate School of Science and Technology, Kumamoto University, 2-39-1 Kurokami, Chuo-ku, Kumamoto 860-8555 (Japan). E-mail: hayami@sci.kumamoto-u.ac.jp (S. Hayami)

<sup>b</sup> School of Chemistry, The University of Sydney, NSW 2006, Australia

<sup>c</sup> Institute of Pulsed Power Science (IPPS), Kumamoto University, 2-39-1 Kurokami, Chuo-ku, Kumamoto 860-8555, (Japan).

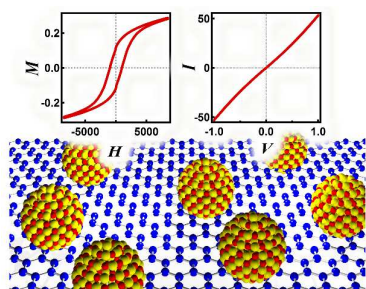
<sup>d</sup> CREST, JST, 7 Gobancho, Chiyoda-ku, Tokyo, 102-0076, (Japan).

† Electronic Supplementary Information (ESI) available: FT-IR, Raman spectra and XPS data. See DOI: 10.1039/c000000x/

- 1 E. Coronado, J. R. Galán-Mascarós, C. J. Gómez-García, V. Laukhin, *Nature*, 2000, **408**, 447.
- 2 E. Ojima, H. Fujiwara, K. Kato, H. Kobayashi, *J. Am. Chem. Soc.*, **1999**, 121, 5581.
- 3 E. Coronado, C. Marti-Gastaldo, E. Navarro-Moratalla, A. Ribera, S. J. Blundell, P. J. Baker, *Nat. Chem.*, 2010, **2**, 1031.
- 4 W. Han, K. M. McCreary, K. Pi, W. H. Wang, Y. Li, H. Wen, J. R. Chen, R. K. Kawakami, *Journal of Magnetism and Magnetic Materials*, 2012, **324**, 369.
- 5 Y. Matsumoto, M. Koinuma, S. Ida, S. Hayami, T. Taniguchi, K. Hatakeyama, H. Tateishi, Y. Watanabe, S. Amano, *J. Phys. Chem. C*, 2011, **115**, 19280.
- 6 M. R. Karim, H. Shinoda, M. Nakai, K. Hatakeyama, H. Kamihata, T. Matsui, T. Taniguchi, M. Koinuma, K. Kuroiwa, M. Kurmoo, Y. Matsumoto, S. Hayami, *Adv. Funct. Mater.*, 2013, **23**, 323.
- 7 K. S. Novoselov, A. K. Geim, S. V. Morozov, D. Jiang, Y. Zhang, S. V. Dubonos, I. V. Grigorieva, A. A. Firsov, *Science*, 2004, **306**, 666.
- 8 R. F. Service, *Science*, 2009, **324**, 875.
- 9 A. K. Geim, *Science*, 2009, **19**, 1530
- 10 G. Eda, G. Fanchini, M. Chhowalla, *Nature Nanotechnology*, 2008, **3**, 270.
- 11 S. Gilje, S. Han, M. Wang, K. L. Wang, R. B. Kaner, *Nano Letters*, 2007, **7**, 3394
- 12 G. Williams, B. Seger, P. V. Kamat, *ACS Nano*, 2008, **2**, 1487.
- 13 K. Nakada, M. Fujita, *Physical Review B*, 1996, **54**, 17954.
- 14 M. Fujita, K. Wakabayashi, K. Nakada, K. Kusakabe, *Journal of the Physical Society of Japan*, 1996, **65**, 1920.
- 15 K. Wakabayashi, M. Fujita, H. Ajiki, M. Sigrist, *Physical Review B*, 1999, **59**, 8271.
- 16 A. R. Armstrong, P. G. Bruce, *Nature*, 1996, **381**, 499.

- 17 M. Baldi, E. Finocchio, F. Milella, G. Busca, *Appl. Catal. B*, 1998, **16**, 43.
- 18 G. C. Milward, M. J. Calderón, P. B. Littlewood, *Nature*, 2005, **443**, 607.
- 19 W. S. Seo, H. H. Jo, K. Lee, B. Kim, S. J. Oh, J. T. Park, *Angew. Chem. Int. Ed.*, 2004, **43**, 1115.
- 20 M. R. Karim, K. Hatakeyama, T. Matsui, H. Takehira, T. Taniguchi, M. Koinuma, Y. Matsumoto, T. Akutagawa, T. Nakamura, S. Noro, T. Yamada, H. Kitagawa, S. Hayami, *J. Am. Chem. Soc.*, 2013, **135**, 8097.
- 21 J. Oh, J. Lee, J. C. Koo, H. R. Choi, Y. Lee, T. Kim, N. D. Luong, J. Nam, *J. Mater. Chem.*, 2010, **20**, 9200; A. S. K. Kumar, N. Rajesh, *RSC Adv.*, 2013, **3**, 2697.
- 22 M. Sakata, A. Funatsu, S. Sonoda, T. Ogata, T. Taniguchi, Y. Matsumoto, *Chem. Lett.*, 2012, **41**, 1625.
- 23 F. Tuinstra, J. L. Koenig, *J. Chem. Phys.*, 1970, **53**, 1126.
- 24 A. C. Ferrari, J. Robertson, *Phys. Rev. B*, 2000, **61**, 14095.
- 25 C. Xu, X. Wang, J. Zhu, *J. Phys. Chem. C*, 2008, **112**, 19841.
- 26 M. Koinuma, H. Tateishi, K. Hatakeyama, S. Miyamoto, C. Ogata, A. Funatsu, T. Taniguchi, Y. Matsumoto, *Chem. Lett.*, 2013, **42**, 924.
- 27 S. Stankovich, D. A. Dikin, R. D. Piner, K. A. Kohlhaas, A. Kleinhammes, Y. Jia, Y. Wu, S. T. Nguyen, R. S. Ruoff, *Carbon*, 2007, **45**, 1558.
- 28 B. Seger, P. V. Kamat, *J. Phys. Chem. C*, 2009, **113**, 7990.
- 29 Y. Tan, L. Meng, Q. Peng, Y. Li, *Chem. Commun.*, 2011, **47**, 1172.
- 30 N. Wang, L. Guo, L. He, X. Cao, C. Chen, R. Wang, S. Yang, *Small*, 2007, **3**, 606.

## Table of Contents



The coexistence of electrical conductivity and ferromagnetism has been achieved in a reduced graphene oxide and manganese oxide hybrid (rGO-Mn).